Mat. Res. Soc. Symp. Proc. Vol. 635 © 2001 Materials Research Society

Studies of the Dielectric Constant of Thin Film Bismuth Nanowire Samples Using Optical Reflectometry

M. R. Black[a,e], Y.-M. Lin[a], S. B. Cronin[b], O. Rabin[c], M. Padi[b], M. S. Dresselhaus[a,b,d]
[a]Department of EECS, Massachusetts Institute of Technology, Cambridge, MA
[b]Department of Physics, Massachusetts Institute of Technology, Cambridge, MA
[c]Department of Chemistry, Massachusetts Institute of Technology, Cambridge, MA
[d]Currently on leave from MIT
[e]Electronic mail: mrb@mgm.mit.edu

ABSTRACT

Arrays of 10 to 120 nm diameter single crystalline bismuth nanowires have been formed inside amorphous alumina templates. Since bismuth has a small effective mass compared to other materials, significant quantum mechanical confinement is expected to occur in wires with diameter less than 50nm. The subbands formed by quantum confinement cause interesting modifications to the dielectric function of bismuth. This study measures the dielectric function of bismuth nanowires in an energy range where the effects of quantum confinement are predicted (0.05 to 0.5 eV). Using Fourier transform infrared reflectometry, the dielectric constant as a function of energy is obtained for the alumina/bismuth composite system. Effective medium theory is used to subtract the effect of the alumina template from the measurement of the composite material, thus yielding the dielectric function of bismuth nanowires. A strong absorption peak is observed at $\sim$1000 cm^{-1} in the frequency dependent dielectric function in the photon energy range measured. The dependence of the frequency and intensity of this oscillator on incident light polarization and wire diameter are reviewed. In addition, the dependence of the optical absorption on antimony and tellurium doping of the nanowires are reported.

Introduction

Scientists and engineers use the effects of low dimensions as another means of tailoring a material to a desired application [1, 2, 3, 4]. In order for the design of a material to be optimized, the key parameters of the low dimensionality need to be measured and compared to theoretical calculations. This paper expands on previous work of looking at quantum confinement in bismuth nanowires by optical reflection.

Bismuth is an ideal material for quantum confinement studies. First of all, when a material's size approaches the de Broglie wavelength of its free carriers, the carriers become quantum confined. The electron and hole energy bands then split into subbands characteristic of a low dimensional material. For a given sample size, the energy separation of these subbands increase as the carriers' effective mass decreases. Since bismuth has small electron and hole effective mass tensors at the L-point (the mass components $\mathbf{m}^*$ vary from 0.001 m_0 to 0.26 m_0 depending on the crystalline direction), the separation between subbands is significant even at sample dimensions as large as $\sim$40 nm. Bismuth also has a large mean free path, $\sim$ 250 nm at 300 K[5], which in addition to the small effective mass is required for quantum confinement. As a result of the small effective mass and the large carrier mean free path, bismuth exhibits quantum confinement at manufacturable dimensions. Furthermore, bismuth has a low melting point ($\sim$271°C), which enables the fabrication of nanowires using

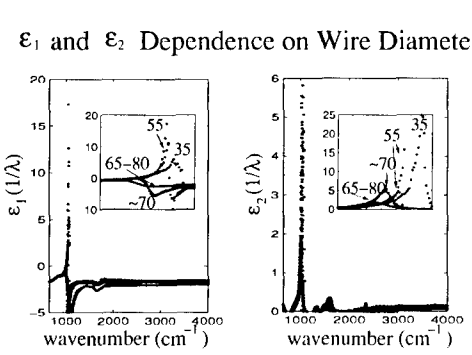

Figure 1: The wire diameter dependence of the dielectric function $(\epsilon_1 + i\epsilon_2)$ of bismuth nanowires vs. wavenumber $(1/\lambda\,\mathrm{cm}^{-1})$ obtained from analysis of reflectivity measurements as reported in reference [7]. Results for samples 1-4 are shown.

a pressure injection technique. Lastly, bismuth nanowires are especially interesting because they exhibit a transition from a semi-metal with a small band overlap (38 meV at 0 K) to a narrow gap semiconductor as the wire diameter decreases and the quantum confinement energy increases [6]. This transition occurs in Bi nanowires at relatively large wire diameters because of its small band overlap and small effective mass tensor. For example, theoretical calculations predict this transition at a wire diameter of 48 nm for wires in the growth direction of our nanowires (< 202 >). The transistion from a semimetal to a semiconductor has significant effects on the electronic, thermoelectric, and optical properties of bismuth, particulary at low temperatures.

In a material that is quantum confined in two dimensions (quantum wires), the electronic joint density of states has a singularity at each energy corresponding to an intersubband transition. If the transition is allowed, incident light at this energy may be strongly absorbed. In a previous study, a strong narrow absorption peak is observed at $\sim$1000 cm^{-1} in bismuth nanowires [7]. In this previous study, the absorption energy is shown to increase as the wire diameter is decreased [7]. These results are reshown in Fig. 1. Since the energy separation of the electronic bands increases with decreasing wire diameter, the observed trend is qualitatively consistent with theory for intersubband transitions. In addition, the polarization dependence of the reflection is presented in this previous study and is also shown in Fig. 2. The features in the reflection at $\sim$1000 cm^{-1} disappear as the electric field is polarized along the direction of the wires. This paper further studies the strong absorption at $\sim$1000 cm^{-1} in bismuth nanowires by investigating the effect of antimony and tellurium doping.

Experimental Details

The bismuth nanowires in this study are fabricated by filling porous alumina with molten bismuth under a high pressure atmosphere [8, 9]. Since the alumina is a wide-bandgap semiconductor, the wires are isolated from each other and the free carriers are confined inside the wire. Porous anodic aluminum oxide templates are fabricated by anodizing aluminum sheets in an oxalic acid solution [8]. During this process, cylindrical pores 7-200 nm in

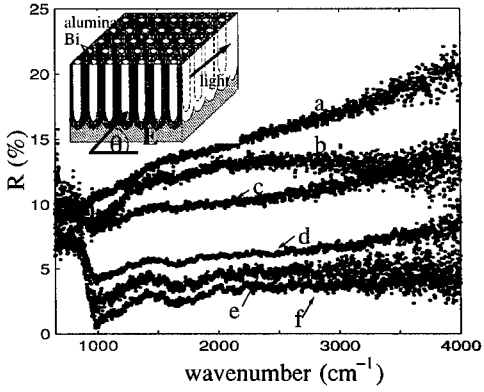

Figure 2: The polarization dependence of the reflection spectra of bismuth nanowires as a function of wavenumber ($1/\lambda\,\mathrm{cm}^{-1}$) as reported in reference [7]. Results for sample 1 is shown.

Table 1: Sample processing conditions

sample	voltage (volts)	temperature (K)	wire diameter (nm)	purity of Bi used to fill template(%)	dopant type	%in melt
1	60	273	65-80	99.99	none	0
2	60	275	~70	99.999	none	0
3	40	290	55	99.999	none	0
4	35	273	35	99.999	none	0
5	45	273	55	99.9999	Sb	15
6	45	273	55	99.9999	Te	0.0189
7	45	273	55	99.9999	Te	0.044
8	45	273	55	99.9999	Te	0.090

diameter are self-assembled into a hexagonal array, as previously reported [8, 9]. The process conditions used in this study are listed in Table 1.

The optical reflection $R(\omega)$ and transmission $T(\omega)$ are measured as a function of frequency at room temperature using a Nicolet Magna-IR 860 spectrometer and the Nic-Plan IR Microscope. Reflection data are taken in the infrared region from $650 < 1/\lambda < 4000\,\mathrm{cm}^{-1}$ at 293 K using a gold film as a comparison standard. The wavenumber resolution is $4\,\mathrm{cm}^{-1}$. Kramers Kronig relations are used to obtain the frequency dependence of the dielectric function of the composite material. Then from the dielectric function of the composite material and using effective medium theory, the dielectric function of the bismuth nanowires is obtained. Effective medium theory is required to separate the bismuth nanowire and alumina host contributions of the total dielectric function since in the frequency range of our experiments, the wavelength of light is more than 50 times greater than the wire diameter and the optical properties of the template and bismuth nanowires are measured simultaneously [10, 11, 12, 13].

Antimony Doping Dependence

Alloying crystalline bismuth with antimony adjusts the L-point bandgap. As the antimony concentration is increased from 0% to 4%, the bandgap decreases from $10meV$ to $0meV$. As the doping is increased further, the band gap continuously increases until pure antimony is reached and the bandgap is $200meV$ [14, 15]. A bismuth - antimony alloy wire was formed by introducing antimony into the melt and then using the same high pressure injection technique as for the pure bismuth wires to inject the alloyed metal into the alumina. The melt contained 15% antimony and 85% bismuth. Since the antimony concentration in the melt is not necessarily the same concentration as inside the nanowires, and furthermore since the nanowires may not have uniform doping along the wire axis, the ratio of antimony to bismuth must be measured after nanowire formation. Electron Dispersive Spectroscopy(EDS) was used to try to measure the concentration of antimony in the as grown sample. However, no antimony was detected. Therefore the concentration and distribution of antimony in the sample is currently unknown.

Although the exact antimony - bismuth ratio inside the nanowires is not known, the absorption peak behaves as expected with the addition of antimony. Fig. 3 shows that the nanowires formed from the 15% antimony melt have an absorption peak with higher energy than either the $35nm$ or $55nm$ undoped bismuth wires. If the sample were pure bismuth, the absorption would be expected to occur close to the $55nm$ undoped peak and below the $35nm$ undoped peak.

Tellurium Doping Dependence

Tellurium impurities are incorporated into our nanowires during the melt process. Concentrations of 0.090, 0.044, 0.018, and 0 weight percent are used. Again EDS is unable to measure impurity concentrations in the final sample. The samples are therefore referred to as heavily doped, lightly doped, very lightly doped, and undoped respectively.

Tellurium impurities in crystalline bismuth act as electron donors, and increase the Fermi energy to account for the increase in electron concentration. Tellurium dopants may also

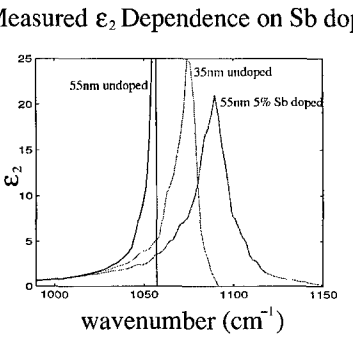

Figure 3: The effect of antimony doping on the absorption peak observed in the dielectric function $(\epsilon_1 + i\epsilon_2)$ of bismuth nanowires vs. wavenumber $(1/\lambda\ \mathrm{cm}^{-1})$ obtained from analysis of reflectivity measurements. Without doping, the 55nm wires are expected to have an absorption peak close to the 55nm undoped wires and below the 35nm undoped wires. However, the doped sample has a peak above both the undoped 35nm and undoped 55nm, demonstrating an increase in bandgap with addition of antimony. Results for samples 3,4, and 5 are shown.

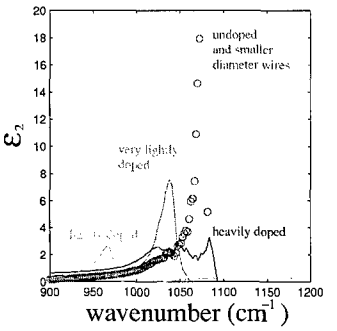

Figure 4: The effect of tellurium doping on the absorption peak observed in the dielectric function $(\epsilon_1 + i\epsilon_2)$ of bismuth nanowires vs. wavenumber $(1/\lambda\ \mathrm{cm}^{-1})$ obtained from analysis of reflectivity measurements. Results for samples 3, 6, 7, and 8 are shown.

decrease τ the average time between scattering events, hence decreasing the coherence length, and thereby decreasing the quantum effects. Only considering the increase in Fermi energy, we expect that at higher doping levels the lower conduction subbands will become more occupied with electrons. When the conduction band is completely filled with electrons, an optical transition from the valence band to the conduction band is forbidden by the Pauli exclusion principal. Therefore, as the doping increases, the higher energy bands dominate the optical spectra. Since bismuth has a strongly coupled valence and conduction band at the L-point, the bands are highly non-parabolic. The intersubband transition is therefore expected to decrease and then increase as the Fermi energy is increased (at $0K$). This is approximately what is observed in Fig. 4. However since the doping is unknown at this time, it is premature to conclude as to the cause of the shift in absorption peak due to the tellurium doping.

Summary

This study reports the effect of tellurium and antimony doping on the absorption peak observed in bismuth nanowires at $\sim$1000 cm^{-1}. The change in the absorption upon doping with either antimony or tellurium confirm that this absorption is from the bismuth nanowires and furthermore show that dopant is incorporated into the nanowires. When antimony is incorporated into the nanowires, the energy of the peak absorption increases. This increase is consistent with the increase in the bandgap of bulk bismuth - antimony alloys with increasing antimony doping. The peak energy changes non-monotonically with increasing doping of tellurium. More work is needed to determine the cause of this non-monotonic increase.

Acknowledgements

The authors gratefully acknowledge the assistance of Mellisa Sanders, and Gene Dresselhaus The authors gratefully acknowledge MURI subcontract 0205-G-7A114-01, NSF grant DMR-98-04734, and US Navy contract N00167-92-K005 for support. This work made use of MRSEC Shared Facilities supported by the National Science Foundation contract DMR-9400334.

References

[1] N. Kouklin, S. Bandyopadhyay, S. Tereshin, A. Varfolomeev, and D. Zaretsky, Applied Physics Letters **76**, 460–519 (2000).

[2] D. E. Aspnes, A. Heller, and J. D. Porter, J. Appl. Phys. **60**, 3028–3034 (1986).

[3] M. S. Dresselhaus, T. Koga, X. Sun, S. B. Cronin, K. L. Wang, and G. Chen. In *Sixteenth International Conference on Thermoelectrics: Proceedings, ICT'97; Dresden, Germany*, edited by Armin Heinrich and Joachim Schumann, pages 12–20, Institute of Electrical and Electronics Engineers, Inc., Piscataway, NJ 09955-1331, 1997. IEEE Catalog Number 97TH8291; ISSN 1094-2734.

[4] L. D. Hicks and M. S. Dresselhaus, Phys. Rev. B **47**, 12727–12731 (1993).

[5] V. Damodara Das and N. Soundararajan, Phys. Rev. B. **35**, 5990–5996 (1987).

[6] Y. M. Lin, X. Sun, and M. S. Dresselhaus, Phys. Rev. B **62**, 4610–4623 (2000).

[7]

[8] M. R. Black, M. Padi, S. Cronin, Y.-M. Lin, O. Rabin, T. McClure, G. Dresselhaus, P. L. Hagelstein, and M. S. Dresselhaus, Appl. Phys. Lett.**75** (2000).

[9] Z. Zhang, J. Ying, and M. Dresselhaus, J. Mater. Res. **13**, 1745–1748 (1998).

[10] J. Heremans, C. M. Thrush, Y. Lin, S. Cronin, Z. Zhang, M. S. Dresselhaus, and J. F. Mansfield, Physical Review B **61**, 2921–2930 (2000).

[11] G. L. Hornyak, C. J. Patrissi, and C. R. Martin, J. Phys. Chem. B. **101**, 1548–1555 (1997).

[12] C. A. Foss, Jr. G. L. Hornyak, J. A. Stockert, and C. R. Martin, J. Phys. Chem. B. **98**, 2963–2971 (1994).

[13] D. E. Aspnes, Thin Solid Films **89**, 249–262 (1982).

[14] N. L. Cherkas, Opt. Spectrosc. **81**, 906–912 (1996).

[15] B. Lenoir, A. Dauscher, X. Devaux, R. Martin-Lopez, Yu.I.Ravich, H. Scherrer, and S. Scherrer. In *Fifteenth International Conference on Thermoelectrics: Proceedings, ICT '96*, pages 1–13, Institute of Electrical and Electronics Engineers, Inc., Piscataway, NJ 09955-1331, 1996.

[16] H. J. Goldsmid, Phys. Stat. Sol. **1**, 7–28 (1970).